ORIGINAL ARTICLE

Synthesis and crystal structure of dehydrated, deaminated, and dealuminated zeolite Y (FAU): single-crystal structure of |Na$_{33}$H$_{26}$(Al$_5$O$_4$)|[Si$_{126}$Al$_{66}$O$_{384}$]-FAU

Woo Taik Lim · Sung Man Seo · Oh Seuk Lee ·
Lianzhou Wang · Gao Qing Lu

Abstract A single crystal of zeolite Y, |Na$_{71}$|[Si$_{121}$Al$_{71}$O$_{384}$]-FAU, was ion exchanged to generate |(NH$_4$)$_{38}$Na$_{33}$|[Si$_{121}$Al$_{71}$O$_{384}$]-FAU. This was then vacuum dehydrated at 673 K, and, without re-exposure to the atmosphere, its structure was determined crystallographically using synchrotron X-radiation in the cubic space group $Fd\bar{3}m$ at 294 K. It was refined to the final error index $R_1 = 0.0532$ with 522 reflections for which $F_o > 4\sigma(F_o)$. The composition (best integers) is determined to be |Na$_{33}$H$_{26}$(Al$_5$O$_4$)|[Si$_{126}$Al$_{66}$O$_{384}$]-FAU which means full dehydration, deamination, and dealumination were achieved. The 33 Na$^+$ ions per unit cell were found at two crystallographically distinct positions: nine at site I (in the centers of the D6Rs) and 24 at site II (in supercages opposite S6Rs). The 2.5 sodalite units contained a dimeric tetrahedral aluminate cation (Al–O = 1.40(8) and 1.60(8) Å) at its center. Each [Al$_5$O$_4$]$^{7+}$ cation coordinates to framework oxygen of D6Rs with tetrahedral manner. This work demonstrates that it is possible to obtain large amount of dealuminated species within the H-Y zeolite framework which should enhance the acidity of adjacent sites for higher catalytic activity.

W. T. Lim (✉) · S. M. Seo · O. S. Lee
Department of Applied Chemistry, Andong National University, Andong 760-749, Korea
e-mail: wtlim@andong.ac.kr

L. Wang · G. Q. Lu
ARC Centre of Excellence for Functional Nanomaterials, School of Engineering and Australian Institute for Bioengineering and Nanotechnology, The University of Queensland, Brisbane, QLD 4072, Australia

Introduction

Zeolites are crystalline microporous materials with tetrahedral framework structures enclosing cavities occupied by cations and (unless fully dehydrated) water molecules, both of which have enough freedom of movement to permit cation exchange and reversible dehydration [1]. Zeolites possess many beneficial characteristics including a high cation exchange ability, a well-defined molecular structure, a well-arranged crystalline structure, acidic and thermal stability, high adsorbability, and shape selectivity. They have a wide range of applications including adsorption and catalysis.

In particular, the H$^+$-exchanged form of zeolite is one of the most important catalysts in the hydrocracking process for producing valuable petroleum products from heavy oils. In hydrocracking, Y-type zeolite-based catalysts have many advantages including high activity, low coke formation, high resistance against nitrogen compounds, and high regenerability over amorphous SiO$_2$–Al$_2$O$_3$ catalysts [2]. Acid catalysts, furthermore, especially H$^+$-exchanged zeolites Y (H-Y), are gaining importance in the field of fine chemicals and intermediates together with ZSM-5 zeolites [3].

H-Y zeolite has both Bronsted and Lewis acid sites. The former arises readily from the deamination (loss of NH$_3$) of NH$_4^+$ ions in the NH$_4^+$-exchanged zeolite; the latter are provided by aluminum ions that leave the zeolite framework (dealumination) by steaming at higher temperatures.

The structures of several NH$_4^+$-exchanged A (LTA) and X (FAU) zeolites have been reported [4–8]. McCusker et al. studied the structure of fully dehydrated, fully NH$_4^+$-

exchanged zeolite A [4]. Their single crystal was prepared by a flow method and evacuation at 298 K, which resulted in the complete dehydration of NH$_4$-A with no NH$_4^+$ decomposition. Lee et al. reported the structures of NH$_4^+$, hydrolyzed-Cu^{2+} forms of zeolite A to find the Cu^{2+} positions [5]. Patalinghug et al. studied a structure of Ni^{2+}- and NH$_4^+$-exchanged zeolite X, allowed it to react with HgCl$_2$ vapor at 388 K, and determined the resulting structure [6]. Zhen et al. prepared anhydrous NH$_4^+$-exchanged zeolite X, allowed it to react with HgCl$_2$ vapor at 388 K, and determined the resulting structure [7, 8].

The presence of tetrahedral aluminosilicate species in zeolites A and Y have been suggested by diffraction techniques [8, 9]. Pluth et al. studied the single-crystal structure of Sr^{2+}-exchanged zeolite A and reported the presence of Al complex (AlO$_4$ species) in the center of the sodalite unit with tetrahedral arrangement [9]. Parise et al. determined the structure of zeolite Y treated with NH$_3$/steam and gaseous SiCl$_4$ by neutron powder diffraction techniques. They also found a four coordinated Al species in the center of the sodalite unit [10].

Even though the knowledge of the three-dimensional structures of zeolites is quite important to understand their catalytic properties—which are sensitive to the nature of the cations, their number, and the distribution in the framework cavities—there have been few reports about the accurate crystallographic observation of the dealuminated species within the H-Y zeolite, mainly because H-Y zeolite is extremely active and unstable at elevated temperatures.

Recently, we reported a detailed structural study of the deamination and dealumination processes [11]. We investigated the dehydration, deamination, and dealumination processes in NH$_4^+$-exchanged zeolite Y without steaming as a function of evacuation temperature and reported the positions of the NH$_4^+$ and nonframework Al^{3+} ions.

This work aims to investigate the three-dimensional structure of the progressively deaminated zeolite Y dehydrated at 673 K by the single-crystal X-ray diffraction method at ambient temperature. It is expected that there would be more the dealuminated species formed within zeolite Y. These species, their positions, and their structures were studied crystallographically.

Experimental section

Synthesis of large single crystals of zeolite Y (FAU)

Large colorless single crystals of sodium zeolite Y, stoichiometry |Na$_{71}$|[Si$_{121}$Al$_{71}$O$_{384}$]-FAU, were synthesized from gels of composition 3.58SiO$_2$:2.08NaAlO$_2$:7.59NaOH:455 H$_2$O:5.06TEA:1.23TCl [11–13]. A starting gel was prepared from fumed silica (99.8%, Sigma), sodium aluminate

(technical, Wako), sodium hydroxide (96%, Wako), triethanolamine (TEA, 99+ %, Acros), bis(2-hydroxyethyl) dimethylammonium chloride (TCl, 99%, Acros), and distilled water. Further details are available [11].

Ion-exchange of zeolite Y (FAU)

In contrast to our earlier work, where complete K$^+$-exchange was carried out to maximize NH$_4^+$-exchange of Na-Y [11], in this study K$^+$-exchange was not carried out initially in order to maximize the amount of dealuminated species in the framework of zeolite Y without decreasing crystallinity.

Crystals of hydrated |(NH$_4$)$_{71}$|[Si$_{121}$Al$_{71}$O$_{384}$]-FAU (or (NH$_4$)$_{71}$-Y) were prepared by static ion-exchange of |Na$_{71}$|[Si$_{121}$Al$_{71}$O$_{384}$]-FAU (or Na$_{71}$-Y) with aqueous 0.1 M NH$_4$C$_2$H$_3$O$_2$, pH = 6.9 (Aldrich 99.999%) [11]. A 0.02 g of hydrated sodium zeolite Y was mixed with 15 mL of 0.1 M NH$_4$C$_2$H$_3$O$_2$ in a 15-mL conical tube and then stirred on an orbital shaker (NB-101 M, N-Biotek) for 4 h at room temperature. The NH$_4^+$ ion-exchange procedure was repeated five times with the fresh NH$_4$C$_2$H$_3$O$_2$ solution. The product was then filtered and oven-dried at 323 K for one day. The crystals were found transparent.

Two of these, clear and colorless octahedrons, about 200 μm in cross-section, hydrated NH$_4^+$-exchanged zeolite Y crystals were placed in fine Pyrex capillaries and dehydrated at 673 K and 1.3 × 10^{-4} Pa for 2 days. While these conditions were maintained, the hot contiguous downstream lengths of the vacuum system, including a sequential 17-cm U-tube of zeolite 5A beads fully activated *in situ*, were cooled to ambient temperature to prevent the movement of water molecules from more distant parts of the vacuum system to the crystal. Still under vacuum in their capillaries, the crystals were then allowed to cool and were sealed in their capillaries and removed from the vacuum line by torch. Microscopic examination showed that the resulting single crystals, still under vacuum in their capillaries, were pale yellows.

X-ray diffraction work

X-ray diffraction data of the resulting single-crystals were collected at 294(1) K on an ADSC Quantum210 detector at the Beamline 4A MXW of Pohang Light Source in Korea. Crystal evaluation and data collection were carried out using 0.76999 Å-wavelength radiation with a detector-to-crystal distance of 6.0 cm. Preliminary cell constants and an orientation matrix were determined from 36 sets of frames collected at scan intervals of 5° with an exposure time of 1 s per frame. We obtained the basic scale file from program HKL2000 [14]. The reflections were successfully indexed by the automated

indexing routine of the DENZO program [14]. A total of 165,832 and 169,506 reflections for the each crystal were obtained by collecting 72 sets of frames with $5°$ scans with an exposure time of one second per frame. These highly redundant data sets were corrected for Lorentz and polarization effects, and (negligible) corrections for crystal decay were also applied. The space group $Fd\bar{3}m$ was determined by the program XPREP [15]. A summary of the experimental and crystallographic data is presented in Table 1.

Structure determination

Full-matrix least-squares refinement (SHELXL97) [16] was carried out on F_o^2 using all data. Refinement was initiated with the atomic parameters of the framework atoms [(Si, Al), O(1), O(2), O(3), and O(4)] in dehydrated $|K_{71}|[Si_{121}Al_{71}O_{384}]$-FAU [17]. The initial refinement using anisotropic thermal parameters for all positions converged to the error indices (defined in Table 1 footnote a) $R_1/R_2 = 0.211/0.653$.

Table 2 presents the steps of structure determinations and refinements as new atomic positions were found on successive difference Fourier electron-density functions.

The final cycles of refinement, carried out with the anisotropic temperature factors for all atoms and with the final weighting-scheme parameters, converged to $R_1/R_2 = 0.053/0.203$. The largest peaks appeared on the final difference Fourier function was not included in the final model because they were too far from framework oxygen atoms to be a cation and they were featureless.

All shifts in the final cycles of refinements were less than 0.1% of their corresponding estimated standard deviations. The final structural parameters are given in Table 3. Selected interatomic distances and angles are given in Table 4.

Fixed weights were used initially; the final weights were assigned using the formula $w = 1/[\sigma^2(F_o^2) + (aP)^2 + bP]$ where $P = [\text{Max}(F_o^2, 0) + 2 F_c^2]/3$, with $a/b = 0.083/134.6$ as refined parameters (see Table 1). Atomic scattering factors for N^0, Na^+, O^-, and $(Si, Al)^{1.82+}$ were used [18, 19]. The function describing $(Si, Al)^{1.82+}$ is the weighted mean of the Si^{4+}, Si^0, Al^{3+}, and Al^0 functions assuming half formal charges. All scattering factors were modified to account for anomalous dispersion [20, 21]. The structure was determined again, using a second crystal prepared similar to the first. The second determination was carried out to check reproducibility; only the result for the first crystal is presented in this report (Tables show the data for

Table 1 Summary of experimental and crystallographic data

	First crystal	Second crystal
Crystal cross-section (mm)	0.18	0.19
Ion exchange T (K)	294(2)	294(2)
Ion exchange for NH_4^+ (day, mL)	2, 50	2, 50
Dehydration T (K)	673	673
Crystal color	Pale yellow	Pale yellow
Data collection T (K)	294(1)	294(1)
Space group, Z	$Fd\bar{3}m$, 1	$Fd\bar{3}m$, 1
X-ray source	Pohang light source, Beamline 4A MXW (PLS, 4A MXW BL)	
Wavelength (Å)	0.76999	0.76999
Unit cell constant, a (Å)	24.821(3)	24.819(3)
2θ range in data collection (°)	59.97	59.97
No. of unique reflections, m	932	897
No. of reflections with $F_o > 4\sigma(F_o)$	522	516
No. of variables, s	45	45
Data/parameter ratio, m/s	20.7	19.9
Weighting parameters, a/b	0.083/134.6	0.103/145.1
Final error indices		
R_1/R_2 $(F_o > 4\sigma(F_o))$[a]	0.0532/0.2033	0.0556/0.2251
R_1/R_2 (all intensities)[b]	0.0975//0.2089	0.0987/0.2197
Goodness-of-fit[c]	1.064	1.042

[a] $R_1 = \Sigma|F_o-|F_c||/\Sigma F_o$ and $R_2 = [\Sigma w(F_o^2-F_c^2)^2/\Sigma w(F_o^2)^2]^{1/2}$, R_1 and R_2 are calculated using only the 695 reflections for which $F_o > 4\sigma(F_o)$

[b] R_1 and R_2 are calculated using all unique reflections measured

[c] Goodness-of-fit = $(\Sigma w(F_o^2-F_c^2)^2/(m-s))^{1/2}$, where m and s are the number of unique reflections and variables, respectively

Table 2 Initial steps of structure refinement[a]

Step	Occupancy[b] at					R_1	R_2
	Na(I)	Na(II)	Al(I′)	Al(U)	O(5)		
First crystal							
1[c]						0.2109	0.6534
2		23.9(13)				0.1466	0.5300
3	8.7(6)	21.3(8)				0.0925	0.3326
4	8.6(5)	23.3(7)	9.5(8)			0.0765	0.2837
5	8.8(4)	24.4(6)	12.0(8)	5.1(9)		0.0716	0.2487
6	9.3(4)	24.8(6)	11.3(9)	2.0(8)	8.8(26)	0.0700	0.2464
7	9.0(4)	24.2(5)	11.2(7)	2.9(10)	6.2(23)	0.0527	0.2023
8	9.0	24.0	11.2(7)	2.9(9)	5.9(22)	0.0528	0.2019
9	9.0	24.0	10.1(5)	2.5(1)	10.1(5)	0.0532	0.2056
10	9.0	24.0	10.0	2.5	10.0	0.0532	0.2033
Second crystal							
1[c]						0.2081	0.6511
2		25.3(13)				0.1430	0.5236
3	8.6(6)	20.6(9)				0.0997	0.4457
4	7.9(5)	22.8(7)	9.5(8)			0.0794	0.2880
5	8.2(5)	24.0(7)	12.0(8)	5.2(9)		0.0744	0.2634
6	8.9(5)	24.7(7)	11.5(8)	1.8(7)	10.4(27)	0.0723	0.2567
7	9.0	24.2(6)	11.5(7)	1.9(8)	8.9(24)	0.0608	0.2354
8	9.0	24.0	11.3(7)	2.2(9)	8.2(24)	0.0557	0.2250
9	9.0	24.0	10.5(5)	2.6(1)	10.5(5)	0.0556	0.2254
10	9.0	24.0	10.0	2.5	10.0	0.0532	0.2033

[a] Isotropic temperature factors were used for all Na^+ positions except for the last step

[b] The occupancy is given as the number of Na^+ ions per unit cell

[c] Only the atoms of zeolite framework were included in the initial structure model

both). There were no significant differences between the first and second crystal structure.

Characteristics of the structure

Framework structure

The framework structure of faujasite is characterized by the double 6-ring (D6R, hexagonal prism), the sodalite cavity (a cubooctahedron), and the supercage (see Fig. 1). Each unit cell has eight supercages, eight sodalite cavities, 16 double 6-rings (D6Rs), 16 12-rings, and 32 single 6-rings (S6Rs).

The exchangeable cations, which balance the negative charge of the faujasite framework, usually occupy some or all of the sites shown with Roman numerals in Fig. 1. The maximum occupancies at the cation sites I, I′, II, II′, III, and III′ in faujasite are 16, 32, 32, 32, 48, and (in $Fd\bar{3}m$) 192, respectively. Further description is available [23–25].

Framework and Na^+ ions

In this structure, 33 Na^+ ions were found at two equipoints. The 9 Na^+ ions per unit cell are on 3-fold axes in the D6Rs, at site I. At site II, 24 Na^+ ions were found. The total number of Na^+ ions found per unit cell, 33, differs significantly from 71, the number required to balance the negative charge of the zeolite framework. It is possible that deamination was complete and 38 H^+ ions remained within the zeolite, as has been proposed for the structures of $|(NH_4)_{59}H_5Na_5K_2(H_2O)_3|[Si_{121}Al_{71}O_{384}]$-FAU, $|(NH_4)_{31}H_{33}Na_5K_2|[Si_{121}Al_{71}O_{384}]$-FAU, $|(NH_4)_2H_{62}Na_5K_2|[Si_{121}Al_{71}O_{384}]$-FAU, $|H_{61}Na_5K_2(Al_2O)_{0.5}|[Si_{122}Al_{70}O_{384}]$-FAU, $|H_{53}Na_5K_2(Al_2O)_2|[Si_{124}Al_{68}O_{384}]$-FAU, and $|H_{51}Na_5K_2(Al_2O)_{2.5}|[Si_{124}Al_{68}O_{384}]$-FAU [11].

The 9 Na^+ ions at Na(I) lie at site I, at the center of a D6R (see Fig. 2). Each Na^+ ion at Na(I) coordinates to the six O(3) oxygen atoms of the D6R at a distance of 2.554(6) Å, which is a little longer than the sum of the conventional ionic radii [26] of Na^+ and O^{2-}, 0.97 + 1.32 (respectively) = 2.29 Å, as seen in earlier works [12, 27].

About 24 Na^+ ions are located at site-II positions opposite S6Rs in the supercages (see Figs. 3 and 4). Each of these ions lies inside the supercage, 0.63 Å, from the (111) plane of three O(2) framework oxygens of the S6R to which it is bound (see Table 5). The Na^+ ions are 2.314(6) Å from their nearest neighbors, the O(2) framework oxygens (see Table 4), in close agreement with the sum of the Na^+ and O^{2-} radii [26], 2.29 Å. The O(2)–Na(II)–O(2) angle is 112.89(22)° (see Table 4).

Dealuminated aluminum in the zeolite framework

Following evacuation at 673 K, no NH_4^+ ions remained and a more progressive dealumination of the zeolite framework was observed, compared to our earlier work [11]. With Al^{3+} ions at site I′, U (at the center of the sodalite unit), and oxide ions at site I′, 2.5 tetrahedral $(Al_5O_4)^{7+}$ cations were present per unit cell (see Figs. 3 and 5). Al^{3+} in a 6-ring would be expected to distort that ring appreciably, pulling three framework oxygens close, as was observed in our earlier work [11].

The Al^{3+} ions at Al(I′) are at site I′, on the 3-fold axis in the sodalite unit opposite D6Rs (see Fig. 3). This is 32-fold position, but it is occupied by only 10 Al^{3+} ions. Each Al^{3+} ions at site Al(I′) lies inside the sodalite cavity 0.88 Å from the plane of the O(3) framework oxygens of the D6R which it is bound (see Table 5). Al^{3+} ions at Al(I′) are opposite of 6-ring of some D6Rs. This appears to be the second time that Al^{3+} has been found crystallographically at a conventional ionic site in a zeolite since it was found in our earlier work [11]. It is not an isolated 3-coordinate cation; a bridging oxide ion at the 32-fold axis of Al^{3+} ions at sites

Table 3 Positional, thermal, and occupancy parameters[a]

Atom	Wyckoff position	Cation site	x	y	z	[b]U_{11}	U_{22}	U_{33}	U_{23}	U_{13}	U_{12}	[c]Occupancy		
												Initial	Varied	Fixed
First crystal														
Si, Al	192(i)		−535(1)	1238(1)	359(1)	584(10)	529(10)	529(10)	−43(7)	7(6)	−33(8)	192		
O(1)	96(h)		−1080(2)	0	1080(2)	677(23)	682(35)	677(23)	−81(18)	−89(27)	−81(18)	96		
O(2)	96(g)		−35(2)	−35(2)	1436(2)	626(21)	626(21)	613(33)	−29(18)	−29(18)	77(27)	96		
O(3)	96(g)		−338(3)	687(2)	687(2)	805(41)	672(23)	672(23)	69(29)	71(22)	71(22)	96		
O(4)	96(g)		−672(2)	760(2)	1740(2)	706(36)	666(23)	666(23)	−169(27)	17(21)	−17(21)	96		
Na(I)	16(c)	I	0	0	0	489(28)	489(28)	489(28)	83(33)	83(33)	83(33)		9.0(4)	9
Na(II)	32(e)	II	2315(2)	2315(2)	2315(2)	683(21)	683(21)	683(21)	140(25)	140(25)	140(25)		24.2(5)	24
Al(I′)	32(e)	I′	552(6)	552(6)	552(6)	1185(69)							10.1(5)	10
Al(U)	8(a)	U	1250	1250	1250	2069(320)							2.5(1)	2.5
O(5)	96(g)	I′	878(20)	878(20)	878(20)	2450(389)							10.1(5)	10
Second crystal														
Si, Al	192(i)		−535(1)	1238(1)	359(1)	591(10)	535(10)	537(10)	−49(8)	8(7)	−30(8)	192		
O(1)	96(h)		−1079(2)	0	1079(2)	707(24)	689(36)	707(24)	−76(18)	−98(29)	−76(18)	96		
O(2)	96(g)		−34(2)	−34(2)	1438(2)	622(21)	622(21)	611(34)	−25(18)	−25(18)	75(27)	96		
O(3)	96(g)		−334(3)	688(2)	688(2)	853(44)	664(23)	664(23)	64(30)	63(23)	63(23)	96		
O(4)	96(g)		−673(2)	759(2)	1741(2)	704(37)	673(24)	673(24)	−201(29)	25(22)	−25(22)	96		
Na(I)	16(c)	I	0	0	0	532(31)	532(31)	532(31)	81(36)	81(36)	81(36)		8.9(5)	9
Na(II)	32(e)	II	2318(2)	2318(2)	2318(2)	689(21)	689(21)	689(21)	146(26)	146(26)	146(26)		24.2(6)	24
Al(I′)	32(e)	I′	551(6)	551(6)	551(6)	1074(62)							10.5(5)	10
Al(U)	8(a)	U	1250	1250	1250	2067(330)							2.6(1)	2.5
O(5)	96(g)	I′	878(19)	878(19)	878(19)	2266(360)							10.5(5)	10

[a] Positional parameters $\times 10^4$ and thermal parameters $\times 10^4$ are given. Numbers in parentheses are the estimated standard deviations in the units of the least significant figure given for the corresponding parameter

[b] The anisotropic temperature factor is $\exp[-2\pi^2 a^{-2}(U_{11}h^2 + U_{22}k^2 + U_{33}l^2 + 2U_{23}kl + 2U_{13}hl + 2U_{12}hk)]$

[c] Occupancy factors are given as the number of atoms or ions per unit cell

I′ and U allows each Al^{3+} ion to be 4-coordinate (see Fig. 5). These Lewis acid sites should be very stable because the tetrahedral $(Al_5O_4)^{7+}$ group is protected in a robust setting, the sodalite cage. The Al(I′)–O(3) distance is 2.258(12) Å. This is longer than 1.55 Å, the mean Al–O bond length found in zeolites, because the 6-ring is resisting extreme distortion as seen in our earlier work [11]. The O(3)–Al(I′)–O(3) bond angle is 105.6(7)°.

Ten oxide ions at O(5) lie at site I′ and are recessed 2.29 Å into the sodalite cage from the plane of the O(3) framework oxygens of the D6R which it is bound (see Table 5). The oxide ion is associated with Al^{3+} ion at Al(I′). The Al(I′)-O(5) distance, 1.40(8) Å, is appropriately shorter than 1.65 Å, the mean Al–O bond length found in zeolites. The O(3)–Al(I′)–O(5) bond angle is 113.1(6)° (see Table 4).

The 2.5 Al^{3+} ions occupy site U, at the center of the sodalite unit. The Al(U)–O(5) distance, 1.60(8) Å, agrees well with the mean Al-O bond length found in zeolites. The Al(I′)–O(5)–Al(U) and O(5)–Al(U)–O(5) bond angles are 180° (by symmetry) and 109.47(1)° (see Table 4).

Such a structure, 7+ cationic tetrahedral in a sodalite cage, had only been observed before in zeolite A and X; it was $(In_5)^{7+}$ [28–31]. The smallest organic molecules should be able to reach the Al^{3+} Lewis acid site in the sodalite unit. Accordingly, these sites may be catalytically very active for reactions in petrochemical processes.

Discussion

NH_4^+-exchanged zeolite Y single crystals were evacuated at 673 K, and its structure was determined by X-ray diffraction methods. At this temperature, we observed full dehydration, full deamination, and dealumination. The structure of crystal dehydrated at 673 K could be determined crystallographically without the loss of crystallinity in this work, an advancement from our earlier work [11].

The presence of three-coordinate aluminum in faujasite-type zeolites was suggested by Larson et al. [32], Uytterhoeven et al. [33], and Kuhl et al. [34, 35]. Uytterhoeven et al. especially pointed out the formation of a structure

**Table 4** Selected interatomic distances (Å) and angles (°)[a]

	First crystal	Second crystal
(Si,Al)–O(1)	1.6654(28)	1.6664(30)
(Si,Al)–O(2)	1.6551(22)	1.6566(23)
(Si,Al)–O(3)	1.6651(26)	1.6660(28)
(Si,Al)–O(4)	1.6312(19)	1.6319(20)
Mean (Si,Al)	1.6542(24)	1.6552(25)
Na(I)–O(3)	2.554(6)	2.553(6)
Na(II)–O(2)	2.314(6)	2.310(6)
Al(I′)–O(3)	2.258(12)	2.250(11)
Al(I′)–O(5)	1.40(8)	1.40(8)
Al(U)–O(5)	1.60(8)	1.60(8)
O(1)–(Si,Al)–O(2)	111.31(21)	111.41(22)
O(1)–(Si,Al)–O(3)	107.85(26)	108.09(27)
O(1)–(Si,Al)–O(4)	109.71(27)	109.55(28)
O(2)–(Si,Al)–O(3)	108.17(26)	108.10(27)
O(2)–(Si,Al)–O(4)	106.83(26)	106.64(27)
O(3)–(Si,Al)–O(4)	112.99(29)	113.08(30)
(Si,Al)–O(1)–(Si,Al)	132.0(4)	132.0(4)
(Si,Al)–O(2)–(Si,Al)	142.9(4)	142.5(4)
(Si,Al)–O(3)–(Si,Al)	135.8(4)	135.5(4)
(Si,Al)–O(4)–(Si,Al)	152.7(4)	152.4(4)
O(3)–Na(I)–O(3)	89.58(21), 90.42(21)	89.30(23), 90.70(23)
O(2)–Na(II)–O(2)	112.89(22)	112.62(23)
O(3)–Al(I′)–O(3)	105.6(7)	105.8(7)
O(3)–Al(I′)–O(5)	113.1(6)	113.0(6)
O(5)–Al(U)–O(5)	109.47(1)	109.47(1)
Al(I′)–O(5)–Al(U)[b]	180	180

[a] The numbers in parentheses are the estimated standard deviations in the units of the least significant digit given for the corresponding parameter

[b] Eactly 180° by symmetry

with planar three-coordinate aluminum by reporting the absence of an IR band at about 2,900 cm^{-1} indicated that the pyramidal three-coordinate Bronsted acid form was not present in substantial quantity. Indeed non-framework Al^{3+} at site I′, in this work, coordinates in a nearly trigonal planar manner to three framework oxygens. However it also coordinates axially to one non-framework oxide ion. This oxide ion, O(5) at site I′, bridges linearly between pairs of Al^{3+} ions at site I′ and U to give Al^{3+}-O^{2-}-Al^{3+} groups on the 3-fold axes in some of the sodalite cage.

Deng et al. [36], Ciraolo et al. [37, 38], Seff et al. [39], and Prins et al. [40] found a tetrahedral extra-framework aluminum in faujasite-type zeolites. Deng et al., investigated aluminum species in three dealuminated zeolites (ultrastable HY, HZSM-5 (MFI), and mordenite (MOR)) using the ^{1}H/^{27}Al TRAPDOR method in combination with ^{27}Al MAS NMR [36]. They suggested that the 6.8 ppm signal in the ^{1}H MAS spectra and the 54 ppm signal in the
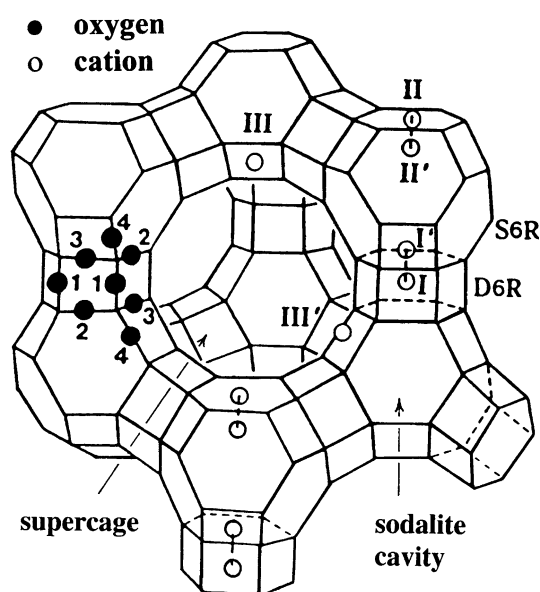

Fig. 1 Stylized drawing of the framework structure of zeolite Y. Near the center of the each line segment is an oxygen atom. The different oxygen atoms are indicated by the numbers 1–4. There is no evidence in this work of any ordering of the silicon and aluminum atoms among the tetrahedral positions, although it is expected that Lowenstein's rule [ref. 22] would be obeyed. Extraframework cation positions are labeled with Roman numerals
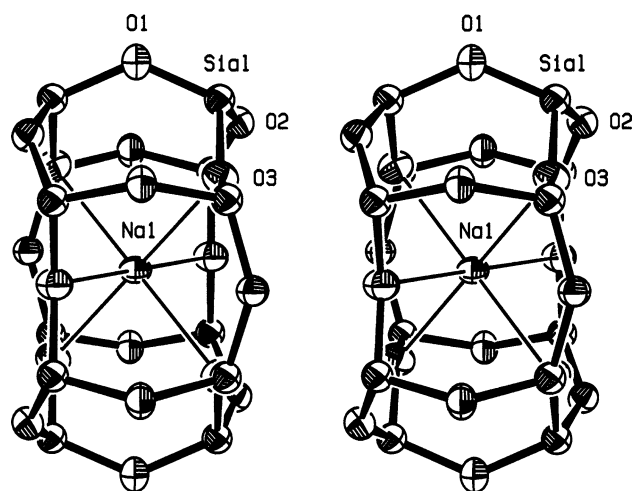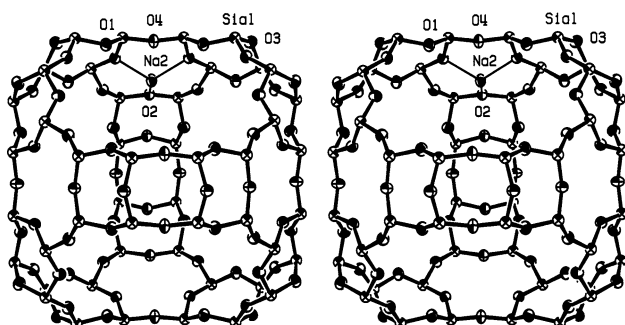

Fig. 2 Stereoview of the representative double 6-rings (D6Rs). The zeolite Y framework is drawn with heavy bonds. The coordination of Na$^+$ ions to oxygens of the zeolite framework are indicated by light bonds. Ellipsoids of 25% probability are shown

^{27}Al MAS spectra of the HY and mordenite zeolites were due to four-coordinate Al^{3+}. The monomeric tetrahedral aluminate ion, AlO$_4$$^{5-}$, had been found in the powder and single-crystal X-ray diffraction work of Ciraolo et al. [37, 38] and Seff et al. [39], respectively, on Zn^{2+}-exchanged FAU-type zeolites. Prins et al. [40] assigned the signals at 0, 30, and 53 ppm in the ^{27}Al NMR spectrum of HZSM-5
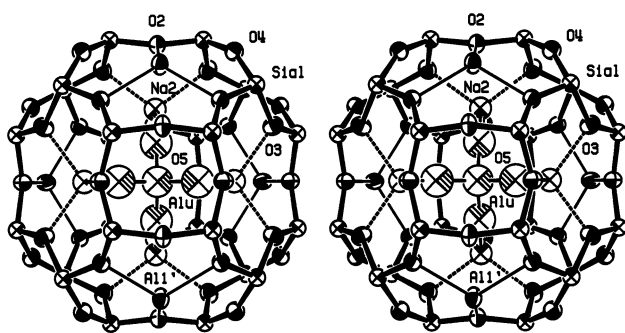
Fig. 3 Stereoview of the representative sodalite units. See the caption to Fig. 2 for other details

Fig. 4 Stereoviews of the representative supercage. See the caption to Fig. 2 for other details

Table 5 Displacements of atoms (Å) from six-ring planes[a]

	Position	Site	First crystal Displacement	Second crystal Displacement
At O(3)[a]	Na(I)	I	1.49	1.49
	Al(I')	I'	−0.88	−0.88
	Al(U)	U	−3.89	−3.88
	O(5)	I'	−2.29	−2.28
At O(2)[b]	Na(II)	II	0.63	0.64

[a] A positive displacement indicates that the ion lies within a D6R. A negative deviation indicates that the ion lies in a sodalite unit

[b] The positive displacement indicates that the ion lies in the supercage

(MFI) to 6-coordinate, highly distorted tetrahedral or 5-coordinate, and tetrahedral Al^{3+}, respectively.

With increasing evacuation temperature, the unit cell constants decreased as found in our previous work [11]. The greater decrease in unit cell constants observed in this work suggests that the framework became richer in Si as Al was lost (see Fig. 6). To maintain its crystallinity, crystal reconstruction occurred to keep the T sites filled.

Kuhl et al. [34] studied the structural stability of Na,NH$_4$-X and found that the faujasite structure is destroyed upon calcination if more than about 32 protons are generated per unit cell. Seff et al. [41] observed that
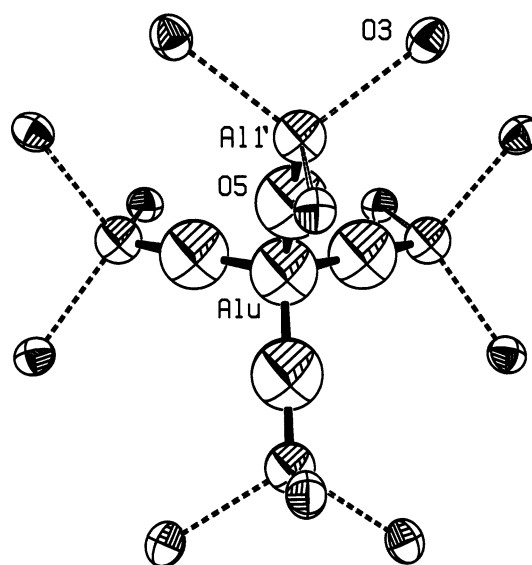
Fig. 5 A $(Al_5O_4)^{7+}$ ions in the sodalite units. The approximately tetrahedral coordination about Al^{3+} can be seen. Ellipsoids of 25% probability are used

Na,H-X (Si/Al = 1.09) containing between 33 and 56 H$^+$ ions maintained good crystallinity. Their separate experiments show that the product zeolite remains highly crystalline at these points. Seff et al. [42] reported that a single crystal of fully La^{3+}-exchanged zeolite X vacuum dehydrated at 400 °C had 92 H$^+$ ions per unit cell; this was possible because a La_2O_3 continuum ($La_{32}O_{48}$ per unit cell) filled all sodalite cavities and D6Rs. They suggested that the protons all associated with oxygens of the anionic zeolite framework and were all in the supercages.

This work shows that zeolite Y, with Si/Al = 1.70, some alkali metal cations, and 26 H$^+$ ions per unit cell, at 673 K, could still exhibit good crystallinity. We have demonstrated that as temperature increases, the unit cell
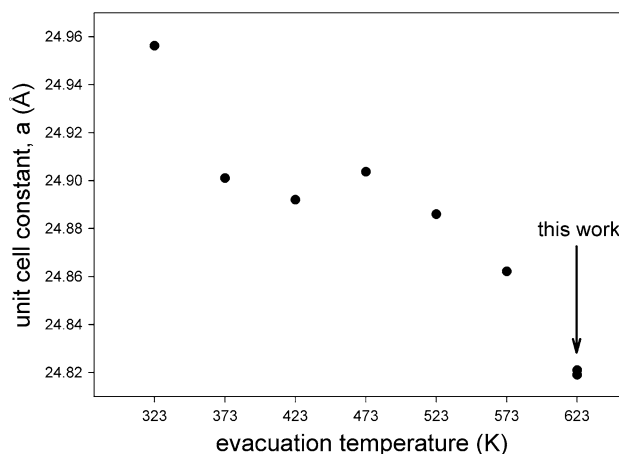
Fig. 6 Unit cell constants as a function of evacuation temperature compared with the data of Ref. [8]

constants decrease significantly. However, due to the crystal reconstruction to keep the T-sites filled, good crystallinity was maintained. Furthermore, we have successfully shown the Lewis acid site in the sodalite unit of zeolite Y, which may be catalytically very active in petrochemical reactions even though we failed to grow single crystals with lower Al content for diffraction experiments to better represent the commercial materials such as ultrastable zeolite Y (USY). The $[Al_5O_4]^{7+}$ group found in this work should enhance the acidity of adjacent sites to give rise to higher catalytic activity.

References

1. Bhatia, S.: Zeolite catalysis. In: Principles and Applications, pp. 1. CRC Press, Inc. Boca Raton, Florida (1988)
2. Sato, K., Nishimura, Y., Honna, K., Matsubayashi, N., Shimada, H.: Role of HY zeolite mesopores in hydrocracking of heavy oils. J. Catal. **200**, 288–297 (2001). doi:10.1006/jcat.2001.3184
3. Anand, R., Khaire, S.S., Maheswari, R., Gore, K.U., Chumbhale, V.R.: N-Alkylation of aniline with ethanol over HY and dealuminated HY zeolites. Appl. Catal. A **242**, 171–177 (2003). doi:10.1016/s0926-860X(02)00502-1
4. McCusker, L.B., Seff, K.: Crystal structure of vacuum-dehydrated fully ammonium-exchanged zeolite A. J. Am. Chem. Soc. **103**, 3441–3446 (1981). doi:10.1021/ja00402a031
5. Lee, H.S., Cruz, W.V., Seff, K.: Crystal structures of solvated $(Cu^{2+})_2(OH^-)_x(NH_4^+)_{8+x}$-A, $_x$ Ca. 2, and partially desolvated $(CuOH^+)_2(NH_4^+)_{10}$-A, zeolite A ion-exchanged with copper(II) from ammonia/water solution. J. Phys. Chem. **86**, 3562–3569 (1982). doi:10.1021/j100215a015
6. Patalinghug, W.C., Seff, K.: Crystal structure of partially desolvated $(NiOH^+)_2(NH_4^+)_{10}$-A, with some discussion of the fully solvated structure. J. Phys. Chem. **94**, 7662–7665 (1990). doi:10.1021/j100382a063
7. Zhen, S., Seff, K.: Crystal structure of anhydrous NH_4^+-exchanged zeolite X partially reacted with $HgCl_2$ vapor. cationic chloromercuric clusters, regular octahedral Hg(II), and regular trigonal Hg(II). J. Phys. Chem. B **103**, 10409–10416 (1999). doi:10.1021/jp9924272
8. Zhen, S., Seff, K., Errata: Crystal structure of anhydrous NH_4^+-exchanged zeolite X partially reacted with $HgCl_2$ vapor. cationic chloromercuric clusters, regular octahedral Hg(II), and regular trigonal Hg(II). J. Phys. Chem. B **105**, 12222 (2001). doi:10.1021/jp9924272
9. Pluth, J.J., Smith, J.V.: Crystal structure of dehydrated Sr-exchanged zeolite A. Absence of near-zero-coordinate Sr^{2+}. Presence of Al Complex. J. Am. Chem. Soc. **104**, 6977–6982 (1982). doi:10.1021/ja00389a015
10. Parise, J.B., Corbin, D.R., Abrams, L.: Structure of dealuminated linde Y-zeolite; $Si_{139.7}Al_{52.3}O_{384}$ and $Si_{173.1}Al_{18.9}O_{384}$: presence of non-framework Al species. Acta Cryst **C40**, 1493–1497 (1984). doi:10.1107/S0108270184008490
11. Lim, W.T., Seo, S.M., Kim, G.H., Lee, H.S., Seff, K.: Six Single-crystal structures showing the dehydration, deamination, dealumination, and decomposition of NH_4^+-exchanged zeolite Y (FAU) with increasing evacuation temperature. Identification of a Lewis acid site. J. Phys. Chem. C **111**, 18294–18306 (2007). doi:10.1021/jp0742721
12. Ferchiche, S., Valcheva-Traykova, M., Vaughan, D.E.W., Warzywoda, J., Sacco, Jr., A.: Synthesis of large single crystals of template Y faujasite. J. Cryst. Growth **222**, 801–805 (2001). doi:10.1016/S0022-0248(00)00979-9
13. Seo, S.M., Kim, G.H., Lee, H.S., Ko, S.O., Lee, O.S., Kim, Y.H., Kim, S.H., Heo, N.H., Lim, W.T.: Single-crystal structure of fully dehydrated sodium zeolite Y (FAU), |Na71|[Si121Al71O384]-FAU. Anal. Sci. **22**, x209–x210 (2006). doi:10.2116/analscix.22.x209
14. Otwinowski, Z., Minor, W.: Processing of X-ray diffraction data collected in oscillation mode. Methods Enzymol. **276**, 307–326 (1997). doi:10.1016/S0076-6879(97)76066-X
15. Bruker-AXS (ver. 6.12), XPREP, Program for the automatic space group determination. Bruker AXS Inc., Madison, Wisconsin, USA (2001)
16. Sheldrick, G.M.: SHELXL97, Program for the refinement of crystal structures. University of Gottingen, Germany (1997)
17. Lim, W.T., Choi, S.Y., Choi, J.H., Kim, Y.H., Heo, N.H., Seff, K.: Single crystal structure of fully dehydrated fully K^+-exchanged zeolite Y (FAU), K71Si121Al71O384. Microporous Mesoporous Mater. **92**, 234–242 (2006). doi:10.1016/j.micromeso.2005.11.052
18. Doyle, P.A., Turner, P.S.: Relativistic Hartree-Fock X-ray and electron scattering factors. Acta Crystallogr. Sect. A **24**, 390–397 (1968). doi:10.1107/S0567739468000756
19. Cromer, D.T., Waber, J.T.: International tables for X-ray Crystallography. vol. IV, pp. 71–98. Kynoch Press, Birmingham, England (1974)
20. Cromer, D.T.: Anomalous dispersion corrections computed from self-consistent field relativistic Dirac-Slater wave functions. Acta Crystallogr. **18**, 17–23 (1965). doi:10.1107/S0365110X6500004X
21. Hamilton, W.C.: International Tables for X-ray Crystallography, vol. IV, pp. 148–150. Kynoch Press, Birmingham, England (1974)
22. Loewenstein, W.: The distribution of aluminum in the tetra-hedra of silicate and aluminates. Am. Mineral. **39**, 92–96 (1954)
23. Smith, J.V.: Molecular sieve zeolites-I. In: Flanigen, E.M., Sand, L.B. (Eds.) Advances in Chemistry Series, vol. 101, pp. 171–200. American Chemical Society Washington, D. C. (1971)
24. Yeom, Y.H., Kim, Y., Seff, K.: Crystal structure of zeolite X exchanged with Pb(II) at pH 6.0 and dehydrated: $(Pb^{4+})_{14}$ $(Pb^{2+})_{18}(Pb_4O_4)_8Si_{100}Al_{92}O_{384}$. J. Phys. Chem. B **101**, 5314–5318 (1997). doi:10.1021/jp970727i
25. Song, M.K., Kim, Y., Seff, K.: Disproportionation of an element in a zeolite. I. Crystal structure of a sulfur sorption complex of dehydrated, fully Cd^{2+}-exchanged zeolite X. Synthesis of tetrahedral S_4^{4+} and n-S_4^{2+}, two new polyatomic cations of sulfur. J. Phys. Chem. B **107**, 3117–3123 (2003). doi:10.1021/jp0215623
26. Chatt, J., L.A. Duncanson, L.A.: Handbook of Chemistry and Physics, 70th edn., pp. F-187. The Chemical Rubber Co., Cleveland, OH (1989/1990)
27. Olson, D.H.: The crystal structure of dehydrated NaX. Zeolites **15**, 439–443 (1995). doi:10.1016/0144-2499(95)00029-6
28. Heo, N.H., Choi, H.C., Jung, S.W., Park, M., Seff, K.: Complete redox exchange of indium for Tl^+ in zeolite A. crystal structures of anhydrous Tl12-A and In10-A·In. Indium appears as In^{2+}, In^+, and In^0. The clusters $(In_5)^{8+}$ and $(In_3)^{2+}$ are proposed. J. Phys. Chem. B **101**, 5531–5539 (1997). doi:10.1021/jp970206v
29. Heo, N.H., Kim, S.H., Choi, H.C., Jung, S.W., Seff, K.: Crystal structures of indium-exchanged zeolite A containing sorbed disulfur. J. Phys. Chem. B **102**, 17–23 (1998). doi:10.1021/jp9715383

30. Heo, N.H., Jung, S.W., Park, S.W., Park, M., Lim, W.T., Seff, K.: Crystal structures of fully indium-exchanged zeolite X. J. Phys. Chem. B **104**, 8372–8381 (2000). doi:10.1021/jp0001992

31. Heo, N.H., Park, J.S., Kim, Y.J., Lim, W.T., Jung, S.W., Seff, K.: Spatially ordered quantum dot array of indium nanoclusters in fully indium-exchanged zeolite X. J. Phys. Chem. B **107**, 1120–1128 (2003). doi:10.1021/jp0219348

32. G. Larson, J.G., Gerberich, H.R., Hall, W.K.: Tracer studies of acid-catalyzed reactions. I. The isomerization of cyclopropane over silica-alumina. J. Am. Chem. Soc. **87**, 1880–1889 (1965). doi:10.1021/ja01087a009

33. Uytterhoeven, J.B., Christner, L.G., Hall, W.K.: Studies of the hydrogen held by solids. VIII. The decationated zeolites. J. Phys. Chem. **69**, 2117–2126 (1965). doi:10.1021/j100890a052

34. Kuhl, G.H., Schweizer, A.E.: Structural stability of sodium ammonium zeolite X. J. Catal. **38**, 469–476 (1975). doi:10.1016/0021-9517(75)90109-8

35. Kuhl, G.H.: The coordination of aluminum and silicon in zeolites as studied by X-ray spectrometry. J. Phys. Chem. Solids **38**, 1259–1263 (1977). doi:10.1016/0022-3697(77)90025-7

36. Deng, F., Yue, Y., Ye, C.: ^{1}H/^{27}Al TRAPDOR NMR studies on aluminum species in dealuminated zeolites. Solid State Nucl. Magn. Reson. **10**, 151–160 (1998). doi:10.1016/S0926-2040(97)00028-3

37. Grey, C.P., Lim, K.H., Norby, P., Ciraolo, M.F.: 12th International Zeolite Conference. Book of Abstracts, abstract P103, Baltimore, Maryland (1998)

38. Ciraolo, M.F., Norby, P., Hanson, J.C., Corbin, D.R., Grey, C.P.: Structural Characterization and Hydrochlorofluorocarbon Reactivity on Zinc-exchanged NaX. J. Phys. Chem. B **103**, 346–356 (1999). doi: 10.1021/jp9834098

39. Bae, D.H., Zhen, S., Seff, K.: Structure of dehydrated Zn^{2+}-exchanged zeolite X. overexchange, framework dealumination and reorganization, stoichiometric retention of monomeric tetrahedral aluminate. J. Phys. Chem. B **103**, 5631–5636 (1999). doi: 10.1021/jp990854+

40. Omega, A., Haouas, M., Kogelbauer, A., Prins, R.: Realumination of dealuminated HZSM-5 zeolites by acid treatment: a reexamination. Microporous Mesoporous Mater. **46**, 177–184 (2001). doi:10.1016/S1387-1811(01)00281-5

41. Zhu, L., Seff, K., Olson, D.H., Cohen, B.J., Von Dreele, R.B.: Hydronium ions in zeolites. 1. Structures of partially and fully dehydrated Na, H_3O-X by X-ray and Neutron diffractions. J. Phys. Chem. B **103**, 10365–10372 (1999). doi:10.1021/jp991070z

42. Park, H.S., Seff, K.: Crystal structures of fully La^{3+}-exchanged zeolite X: an intrazeolitic La_2O_3 continuum, hexagonal planar and trigonally prismatic coordination. J. Phys. Chem. B **104**, 2224–2236 (2000). doi:10.1021/jp992153i